

Steady Flow About A Sphere In A Porous Medium Subject To An Oscillating Temperature

Lai Zhe Phooi¹, Zainodin Haji Jubok², Rozaini Roslan³, Ishak Hashim⁴

^{1,2}School of Science and Technology, Universiti Malaysia Sabah, Jalan UMS,
89400 Kota Kinabalu, Sabah, Malaysia

³Faculty of Science, Arts and Heritage, Universiti Tun Hussein Onn Malaysia,
86400 Parit Raja, Batu Pahat, Johor, Malaysia

⁴Modelling & Data Analysis Research Centre, School of Mathematical
Sciences, Universiti Kebangsaan Malaysia, 43600 Bangi, Selangor, Malaysia

*Corresponding email: zhephooi@gmail.com, zainodin@gmail.com,
rozaini@uthm.edu.my, ishak_h@ukm.my*

Abstract

The study of free convection about a sphere in a porous medium, when the temperature of the sphere is oscillating harmonically is considered for Rayleigh number, $Ra=100$. By using the matched asymptotic expansion, the flow field is divided into an inner region and an outer region, where the inner region is adjacent to the sphere and the outer region is far from the sphere. In the inner region, the separation technique is used to divide the second-order temperature and stream function into steady and unsteady parts. The analytical solution is obtained up to second-order steady term. For outer region, the numerical result up to first order is obtained by using a finite difference scheme. It is found that, a steady flow is induced at the outer edge of the inner region. The temperature and flow patterns are discussed and compared for some frequencies of oscillation, ω and dimensionless parameter ε . It is found that both the magnitudes of temperature and stream functions decreases as ω increases or decreases but the effect of ε is not significant in the outer region. In the inner region, the magnitude of steady flow is also determined by frequency.

Keyword : Steady flow, porous medium, an oscillating temperature

1. INTRODUCTION

In this paper, the study of free convection about a sphere with oscillating temperature in a porous medium is considered. The problem of free convection in porous medium has received much attention from researchers due to its wide applications in the industries such as geothermal systems, groundwater pollutant control, buildings insulation system, nuclear waste design and grain storage. The porous medium such as beach sand, limestone and artificial foam are mainly utilized in diminishing the convection heat transfer that occur around a heated body. It is important to consider the problem with oscillating temperature. However, there is limited literature for the free convection around a sphere in a porous medium where the temperature of the sphere is oscillating harmonically over a mean temperature. The similar problem but in cylindrical case was studied by [1]. A double boundary layer was introduced, and it was found that a steady flow was induced at outside of the inner layer due to the oscillatory temperature.

[2] was the first to consider the free convection about a heated sphere in a porous medium, where the temperature was set to be constant. The analytical solution was found by using a straightforward expansion in terms of a small parameter. Later [5] obtained the solution for spherical problem in porous medium but the temperature is fluctuating over a mean value. The asymptotic expansion was assumed to be steady in the first-order and unsteady in the higher orders and written in terms of an oscillation parameter. [6] investigated the unsteady problem that is suddenly heated and maintains a constant heat flux over the surface. The dimensionless Rayleigh number was assumed small in order to obtain the asymptotic solutions. [7] also considered the unsteady free convection problem in the porous medium for finite value of Rayleigh number, where the case of constant temperature and constant heat flux are solved numerically, while [10] studied the unsteady problem when the surface temperature changes with position. The matched asymptotic expansion was written in terms of small Rayleigh numbers and both steady state solution and transient state solution were presented.

[8] considered the oscillatory free convection in a porous medium for cylindrical case. The result showed that at high frequency, a steady flow persists outside the inner boundary layer. [11] then extended the study of oscillatory free convection about a horizontal cylinder as by [1,4] by proposing a separation method that separates the steady and unsteady term at the second-order solution. A steady flow was induced near the outer edge of the inner region, and this agree with the previous study in [1]. Due to the steady term that dominates

at far from the body with oscillating temperature, this separation technique is direct to the desired result by taking the steady term. Thus motivated by the separation method by [11], the present study is to investigate the oscillatory free convection in a porous medium around a spherical body.

2. MATHEMATICAL FORMULATION

Consider a sphere with radius R_0 immersed in a porous medium with a surrounding temperature, T_∞ . The temperature T'_s of the surface, T'_s , oscillates harmonically over a mean surrounding temperature such that $T'_s = T'_\infty (1 + b \sin a \tau)$, where a is the frequency of oscillation, τ is time, b is the non-dimensional amplitude in temperature oscillations, and the product $T'_\infty b$ is the amplitude of the oscillation. In this study, a spherical polar coordinate system (R, θ, ϕ) is chosen, where R is the radial coordinate, θ is the clockwise angle measured from the vertically upward axis parallel to the gravity acceleration g , and ϕ is the azimuthal angle parallel to the ground. Therefore the problem is reduced into two-dimensional system (R, θ) . The physical system is shown in Fig. 1.

The fluid motion is described by radial and transversal velocity components (U, V) . The velocity component could be expressed in terms of a stream function $\Psi(R, \theta)$ as,

$$U = \frac{1}{R^2 \sin \theta} \frac{\partial \Psi}{\partial \theta} \quad V = -\frac{1}{R \sin \theta} \frac{\partial \Psi}{\partial R} \quad (1)$$

The fluid is assumed to be incompressible and the density of fluid is linear function of temperature. The physical properties are assumed constant and the Boussinesq approximation holds for density variation that is significant only in generating buoyancy force. The porous medium is assumed to be homogeneous, non-deformable, isotropic and the flow is governed by Darcy's law. Additionally, it is assumed that no effect of other heat source such as internal heating and fluid friction.

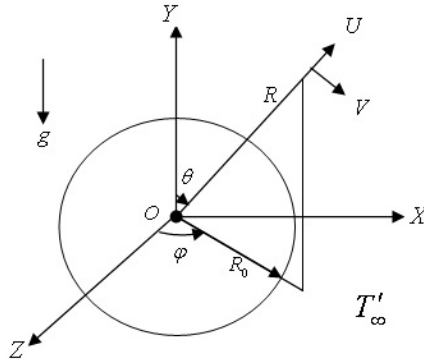


Figure 1. The physical system of the sphere at origin O

The non-dimensional governing equation in terms of the dimensionless temperature T and stream function ψ can be written as

$$\frac{1}{r^2} \frac{\partial}{\partial \theta} \left(\frac{1}{\sin \theta} \frac{\partial \psi}{\partial \theta} \right) + \frac{1}{\sin \theta} \frac{\partial^2 \psi}{\partial r^2} = \cos \theta \frac{\partial T}{\partial \theta} + r \sin \theta \frac{\partial T}{\partial r}, \quad (2)$$

$$\frac{\partial T}{\partial t} + \frac{\varepsilon}{r^2 \sin \theta} \frac{\partial(\psi, T)}{\partial(\theta, r)} = \varepsilon^2 \gamma \left[\frac{1}{r^2} \frac{\partial}{\partial r} \left(r^2 \frac{\partial T}{\partial r} \right) + \frac{1}{r^2 \sin \theta} \frac{\partial}{\partial \theta} \left(\sin \theta \frac{\partial T}{\partial \theta} \right) \right], \quad (3)$$

In which the dimensionless variables are defined as

$$T = \frac{T' - T'_\infty}{T'_\infty b}, \quad \psi = \frac{\Psi}{U_r R_0^2}, \quad r = \frac{R}{R_0}, \quad t = \frac{\tau \alpha}{K \sigma}, \quad (u, v) = \left(\frac{U}{U_r}, \frac{V}{U_r} \right), \quad (4)$$

$$U_r = \frac{g \beta K}{\nu} T'_\infty b, \quad Ra = \frac{R_0 U_r}{\alpha}, \quad \varepsilon = \frac{K U_r}{\alpha R_0}, \quad \gamma = \frac{1}{\varepsilon Ra}, \quad \omega = \frac{a \sigma K}{\alpha}$$

where U_r is the characteristic velocity scale, σ is the heat capacity ratio, g is gravitational acceleration, β is the coefficient of thermal expansion, K is the permeability of porous medium, ν is the kinematic viscosity of fluid, and α is thermal diffusivity of the porous medium. Ra is the Rayleigh number, ε and γ are the dimensionless parameters respectively and ω is the dimensionless frequency.

The boundary conditions necessary for the problem are written as :

$$\psi = 0, T = \sin(\omega t) \quad \text{at} \quad r = 1, \quad (5)$$

$$u \rightarrow 0, v \rightarrow 0, T \rightarrow 0 \quad \text{as} \quad r \rightarrow \infty, \quad (6)$$

$$\frac{\partial u}{\partial \theta} = 0, v = 0, \frac{\partial T}{\partial \theta} = 0 \quad \text{at} \quad \theta = 0, \pi. \quad (7)$$

3. RESULTS

In order to find the approximate solutions to the temperature and stream function, the method of matched asymptotic expansion is appropriate for this problem. The flow domain is divided into two domains i.e. an inner region and an outer region. The problem in the inner region is solved with an analytical approach while the problem in the outer region is solved numerically with Gauss-Seidel iterative method.

3.1 Solution in the inner region

Following the separation technique on the second-order terms as proposed by [11], the asymptotic expansion in the inner region for $T^{(i)}$ and $\psi^{(i)}$ are assumed to be of the form,

$$T^{(i)} = T_0^{(i)}(t, \eta, \theta) + \varepsilon [T_1^{(i)s}(\eta, \theta) + T_1^{(i)u}(t, \eta, \theta)] + \varepsilon^2 T_2^{(i)}(t, \eta, \theta) + h.o.t \quad (8)$$

$$\psi^{(i)} = \varepsilon \psi_0^{(i)}(t, \eta, \theta) + \varepsilon^2 [\psi_1^{(i)s}(\eta, \theta) + \psi_1^{(i)u}(t, \eta, \theta)] + \varepsilon^3 \psi_2^{(i)}(t, \eta, \theta) + h.o.t \quad (9)$$

where the superscripts s and u denote the steady and unsteady parts in second-order terms, respectively. Since the flow near the sphere surface experience larger gradient, the radial coordinate is stretched as

$$\eta = \frac{r-1}{\varepsilon}. \quad (10)$$

Thus substituting equations (8) and (9) into the governing equations, and equating the terms in increasing order of ε , yields the required equation for first-order and second-order equations as

$$\frac{\partial T_0^{(i)}}{\partial t} = \gamma \frac{\partial^2 T_0^{(i)}}{\partial \eta^2}, \quad (11)$$

$$\frac{\partial^2 \psi_0^{(i)}}{\partial \eta^2} = \sin^2 \theta \frac{\partial T_0^{(i)}}{\partial \eta}, \quad (12)$$

$$\gamma \sin \theta \frac{\partial^2 T_1^{(i)s}}{\partial \eta^2} = \left[\frac{\partial(\psi_0^{(i)}, T_0^{(i)})}{\partial(\theta, \eta)} \right]^s, \quad (13)$$

$$\frac{\partial^2 \psi_1^{(i)s}}{\partial \eta^2} = \sin^2 \theta \frac{\partial T_1^{(i)s}}{\partial \eta}, \quad (14)$$

subject to the boundary conditions (5) – (7). From equations (11) and (12) for first-order and equations (13) and (14) for second-order steady term with a superscript s, it could be seen that the first-order terms are time-dependent and the second are left with function of (θ, η) . Then the first order solutions for the above equations are presented as below,

$$T_0^{(i)} = e^{-\sqrt{\frac{\omega}{2\gamma}}\eta} \sin \left(\omega t - \sqrt{\frac{\omega}{2\gamma}}\eta \right), \quad (15)$$

$$\begin{aligned} \psi_0^{(i)} = & \sqrt{\frac{\gamma}{2\omega}} \sin^2 \theta \cos \omega t \left\{ e^{-\sqrt{\frac{\omega}{2\gamma}}\eta} \left[\sin \left(\sqrt{\frac{\omega}{2\gamma}}\eta \right) + \cos \left(\sqrt{\frac{\omega}{2\gamma}}\eta \right) \right] - 1 \right\} \\ & + \sqrt{\frac{\gamma}{2\omega}} \sin^2 \theta \sin \omega t \left\{ e^{-\sqrt{\frac{\omega}{2\gamma}}\eta} \left[\sin \left(\sqrt{\frac{\omega}{2\gamma}}\eta \right) - \cos \left(\sqrt{\frac{\omega}{2\gamma}}\eta \right) \right] + 1 \right\}. \end{aligned} \quad (16)$$

For the second-order steady terms, the solutions for $T^{(i)}$ and $\psi^{(i)}$ are :

$$\begin{aligned} T_1^{(i)s} = & \frac{\cos \theta}{\omega} \left\{ 1 + e^{-\sqrt{\frac{\omega}{2\gamma}}\eta} \left[\sin \left(\sqrt{\frac{\omega}{2\gamma}}\eta \right) - \cos \left(\sqrt{\frac{\omega}{2\gamma}}\eta \right) \right] \right. \\ & \left. - \frac{1}{4} e^{-\sqrt{\frac{2\omega}{\gamma}}\eta} \sin \left(\sqrt{\frac{2\omega}{\gamma}}\eta \right) \right\} + c_1 \eta, \end{aligned} \quad (17)$$

$$\psi_1^{(i)s} = \frac{\sin^2 \theta \cos \theta}{\omega} \sqrt{\frac{2\gamma}{\omega}} \left\{ \frac{1}{16} e^{-\sqrt{\frac{2\omega}{\gamma}} \eta} \left[\cos \left(\sqrt{\frac{2\omega}{\gamma}} \eta \right) + \sin \left(\sqrt{\frac{2\omega}{\gamma}} \eta \right) \right] - e^{-\sqrt{\frac{\omega}{2\gamma}} \eta} \sin \left(\sqrt{\frac{\omega}{2\gamma}} \eta \right) - \frac{1}{16} \right\} + c_2 \sin^2 \theta \eta^2 + c_3 \eta, \quad (18)$$

where c_1 , c_2 and c_3 are constant that could not satisfy the boundary conditions. It will be discussed in the next section.

3.2 Solution in the outer region

In the outer region, the asymptotic expansions for $T^{(0)}$ and $\psi^{(0)}$ are assumed to be of the form

$$T^{(0)} = T_0^{(0)}(\bar{\eta}, \theta) + \sqrt{\varepsilon} T_1^{(0)}(\bar{\eta}, \theta) + \varepsilon T_2^{(0)}(\bar{\eta}, \theta) + h.o.t. \quad (19)$$

$$\psi^{(0)} = \sqrt{\varepsilon} \psi_0^{(0)}(\bar{\eta}, \theta) + \varepsilon \psi_1^{(0)}(\bar{\eta}, \theta) + \varepsilon \sqrt{\varepsilon} \psi_2^{(0)}(\bar{\eta}, \theta) + h.o.t. \quad (20)$$

where the stretched radial coordinate in this region is defined as

$$\bar{\eta} = \frac{r-1}{\sqrt{\varepsilon}}. \quad (21)$$

Similar to the work in the inner region, by substituting expansions (19) and (20) into the governing equations, and equating the terms in increasing order of $\sqrt{\varepsilon}$ yields the required equations for $T_0^{(0)}$ and $\psi_0^{(0)}$ as,

$$\frac{\partial \psi_0^{(0)}}{\partial \theta} \frac{\partial T_0^{(0)}}{\partial \bar{\eta}} - \frac{\partial \psi_0^{(0)}}{\partial \bar{\eta}} \frac{\partial T_0^{(0)}}{\partial \theta} = \gamma \sin \theta \frac{\partial^2 T_0^{(0)}}{\partial \bar{\eta}^2}, \quad (22)$$

$$\frac{\partial^2 \psi_0^{(0)}}{\partial \bar{\eta}^2} = \sin^2 \theta \frac{\partial T_0^{(0)}}{\partial \bar{\eta}}, \quad (23)$$

subject to the matching boundary conditions in the inner edge,

$$\psi^{(0)} \rightarrow -\frac{\sin^2 \theta \cos \theta}{8\omega} \sqrt{\frac{\gamma}{2\omega}}, \quad T^{(0)} \rightarrow \frac{\cos \theta}{\omega}, \quad \text{as } \bar{\eta} \rightarrow 0, \quad (24)$$

and for outer edge, the boundary conditions on $T_0^{(0)}$ and $\psi_0^{(0)}$ are

$$\frac{\partial \psi^{(0)}}{\partial \bar{\eta}} \rightarrow 0, T^{(0)} \rightarrow 0, \quad \text{as } \bar{\eta} \rightarrow \infty. \quad (25)$$

The symmetrical boundary conditions are similar as equation (7). Equations (16) and (17) are now readily solved numerically using a finite difference scheme. The central difference is used to discretize the equations for all interior points. For the Neumann boundary conditions in equations (25) and (7), two-point forward and backward difference are used to formulate the additional equations. The solution is obtained by using Gauss-Seidel iteration method. First, the energy equation (22) which is responsible for generating temperature, is solved at k-th level subject to the boundary conditions. Then, the value for T_{ij}^k is brought into equation (23) for the stream flow. Subsequently the most updated value for ψ_{ij}^k is used to generate the k+1-th level terms for temperature, and so on. The convergence criterion for the iterations is chosen as follows:

$$|\delta_{ij}^k - \delta_{ij}^{k-1}| < \xi \quad (26)$$

where δ is $T^{(0)}$ or $\psi^{(0)}$, and ξ is the maximum error allowed. In this study, the convergence criterion is set to be $\xi=10^{-7}$. The effect of grid resolution is examined in order to determine the appropriate independent mesh size. The value of $\psi^{(0)}$ at $r = 4.0$, $\theta = \pi/5$ is examined as shown in Table 1. The grid independent test is repeated until the changes in test value diminish. Taking into account the number of iteration that needed and the difference of $\psi^{(0)}$ across the grid resolution, the size of $[\bar{\eta}_{\text{grid}} \times \theta_{\text{grid}}] = 401 \times 81$ is appropriate for generating plots.

Table 1. Comparison of $\psi^{(0)}$ at $r = 4.0$, $\theta = \pi/5$ for $\omega = 2$, $\varepsilon = 10^{-1}$ and $\xi = 10^{-7}$.

Ra	(i) Grid resolution and (ii) $\psi^{(0)}$ at $r=4.0$					
	100	(i)	51x11	101x21	201x41	401x81*
	(ii)	0.039383	0.044103	0.044944	0.044760	0.044055

* This grid resolution is used in this study.

4. DISCUSSION

4.1 Flow in the inner region

From the above results, it is clear that $T_0^{(i)}$ and $\psi_0^{(i)}$ are time-dependent. Both $T_0^{(i)}$ and $\psi_0^{(i)}$ are able to satisfy the boundary conditions in the inner region. But for the second-order solutions in equations (17) and (18), $T_1^{(i)s}$ cannot satisfy the boundary condition at the outer edge of the inner region even by setting $c_1=0$. Instead, the solution yields

$$\lim_{\eta \rightarrow \infty} T_1^{(i)s}(\eta, \theta) = \frac{\cos \theta}{\omega}. \quad (27)$$

This value is regarded as the required boundary condition at the inner edge of the outer solution. The result is similar to that of [1, 4, 11] about an infinite horizontal cylinder. Then for $\psi_1^{(i)s}$, if we set $c_2=c_3=0$, then we have

$$\lim_{\eta \rightarrow \infty} \frac{\partial \psi_1^{(i)s}}{\partial \eta}(\eta, \theta) = 0, \quad (28)$$

in which the boundary condition for outer edge can be fulfilled and this is similar to the result by [11]. Also, the value of the steady stream function $\psi^{(i)s}$ must be regarded as the inner boundary conditions for the outer region.

The flow is then compared for the case of Rayleigh number, $Ra=100$. The results are shown correspond to two parameters i.e. ε , range from 10^{-1} to 10^{-3} , and ω , range from 2 to 10. The angular position concerned in the inner region is $\theta=\pi/4$ and the dimensionless time variable is set to $t=1$. The results for first-order terms, second-order steady terms and overall inner region flow are discussed throughout.

Fig. 2(a) shows the changes of first-order temperature $T_0^{(i)}$ due to variation in ε . $T_0^{(i)}$ decreases to surrounding temperature faster as ε decreases. For each decreasing power of ε from 10^{-1} to 10^{-3} , the distance from the sphere to the position that $T_0^{(i)}$ approaches surrounding temperature decreases to $\sqrt{0.1}$ about the original distance. While for $\psi_0^{(i)}$ it is noticed that it increases and achieve a constant value after certain distance and this is determined by ε , where at smaller ε the stream function becomes steady nearer to the wall. However, the magnitude of $\psi_0^{(i)}$ increases 3.162 about the previous value for each decrease of ε , as shown in Fig. 2(b).

Fig. 3(a) and Fig. 3(b) compare the effect of frequency ω on $T_0^{(i)}$ and $\psi_0^{(i)}$. Both the magnitudes of $T_0^{(i)}$ and $\psi_0^{(i)}$ decreases as ω increases. The distance

at which the flow becomes steady also decreases. Since the surface temperature is oscillating, the magnitudes of $T_0^{(i)}$ and $\psi_0^{(i)}$ always change in the direction. The changes in flow is greater for the variation of ω when ω is small compare to larger value of ω .

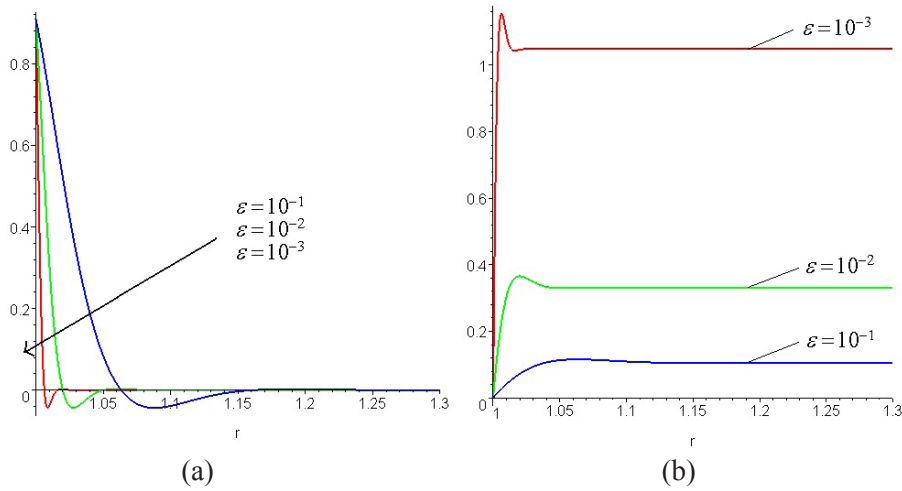


Figure 2. (a) $T_0^{(i)}$ and (b) $\psi_0^{(i)}$ with $t=1$, $\omega=2$, along $\theta=\pi/4$ for various ϵ .

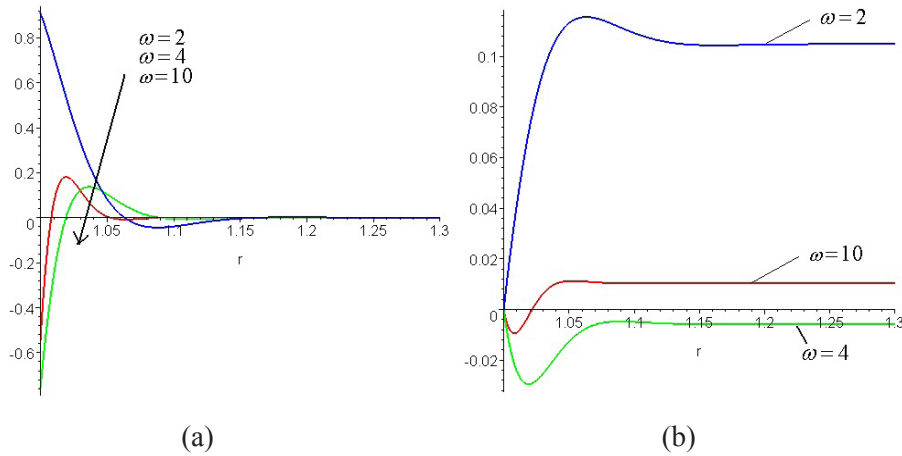


Figure 2. (a) $T_0^{(i)}$ and (b) $\psi_0^{(i)}$ with $t=1$, $\epsilon=10^{-1}$, along $\theta=\pi/4$ for various ω .

In the second-order flow, the effect of ε on $T_1^{(i)s}$ and $\psi_1^{(i)s}$ is shown in Fig. 4(a) and Fig. 4(b), respectively. $T_1^{(i)s}$ increases to a peak value then drops to a steady temperature. This steady temperature and the magnitude of $T_1^{(i)s}$ are independent of ε . But as ε decreases, the steady temperature moves nearer towards the wall. Each decrease of one decimal power, the distance is shortened to $\sqrt{0.1}$ times the original distance. On the other hand, $\psi_1^{(i)s}$ also increases to a peak value, then drops to a steady constant. Unlike $T_1^{(i)s}$, the magnitude of peak and steady constant is determined by ε , where for a decrease of one decimal power, the magnitude of the peak and steady constant are 3.162 about the previous magnitudes. Therefore, at smaller ε , the changes of $\psi_1^{(i)s}$ is greater near the wall but it approaches more rapid to steady state.

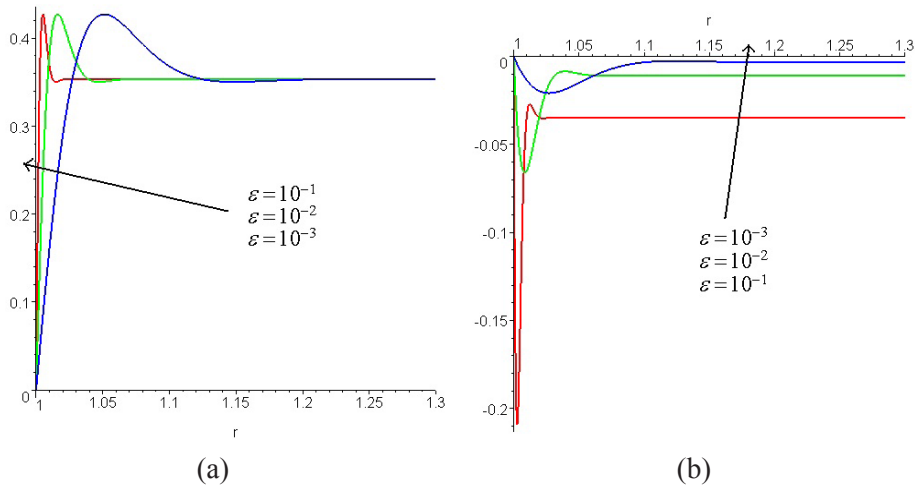


Figure 4. (a) $T_1^{(i)s}$ and (b) $\psi_1^{(i)s}$ with $t=1, \omega=2, \theta=\pi/4$ along for various ε .

The influence of ω are shown in Fig. 5(a) and Fig. 5(b) for $T_1^{(i)s}$ and $\psi_1^{(i)s}$, respectively. It is noted that the increase of ω has the similar effect on both temperature and stream function. The changes of flow at small ω are greater than the changes of flow at large ω . This is because from equation (17) and equation (18), $T_1^{(i)s}$ and $\psi_1^{(i)s}$ is inversely proportional to ω and $\omega^{1.5}$, respectively, hence any changes at small ω is significant to the flow. As ω increases, the magnitude of $\psi_1^{(i)s}$ diminishes faster towards zero. However, in this second-order flow, ω does not change the direction of magnitude but θ .

The overall inner region temperature $T^{(i)}$ is plot for some ε in Fig. 6. is warmer at upper pole and colder at bottom pole. It decreases in all angles for the decrease in ε from 10^{-1} to 10^{-3} . This is result of the dominance of first-order

flow especially when ε is small. For smaller ε , the magnitude of $T^{(i)}$ experiences a rapid drop near the wall and approaches steady temperature. Graph for some values of ε about $\psi^{(i)}$ is shown in Fig. 7. Due to the required boundary condition, the inner stream function executes no flow at the vertical axis, but it reaches a maximum value near the horizontal axis. $\psi^{(i)}$ decrease at all angles as ε decrease. Besides, a very thin closed ring persists near the horizontal axis, where the ring moves towards the wall as ε decrease.

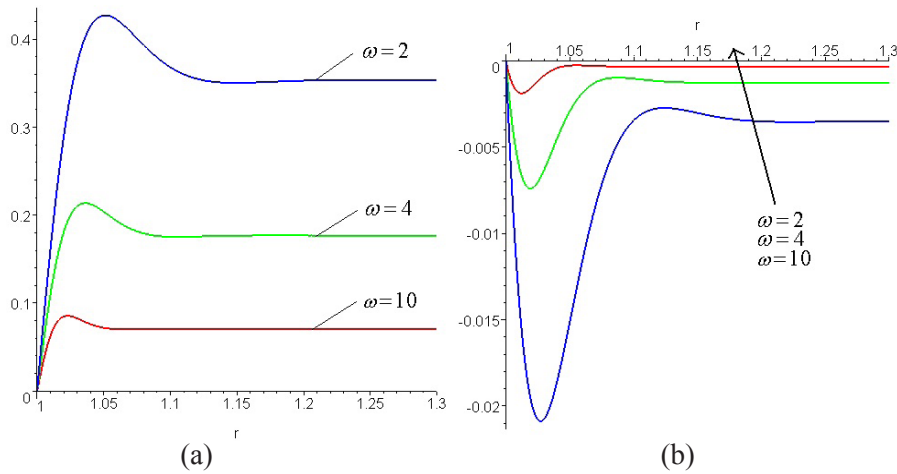


Figure 5. (a) $T_l^{(i)s}$ and (b) $\psi_l^{(i)s}$ with $t=1$, $\varepsilon=10^{-1}$, along $\theta=\pi/4$ for various ω .

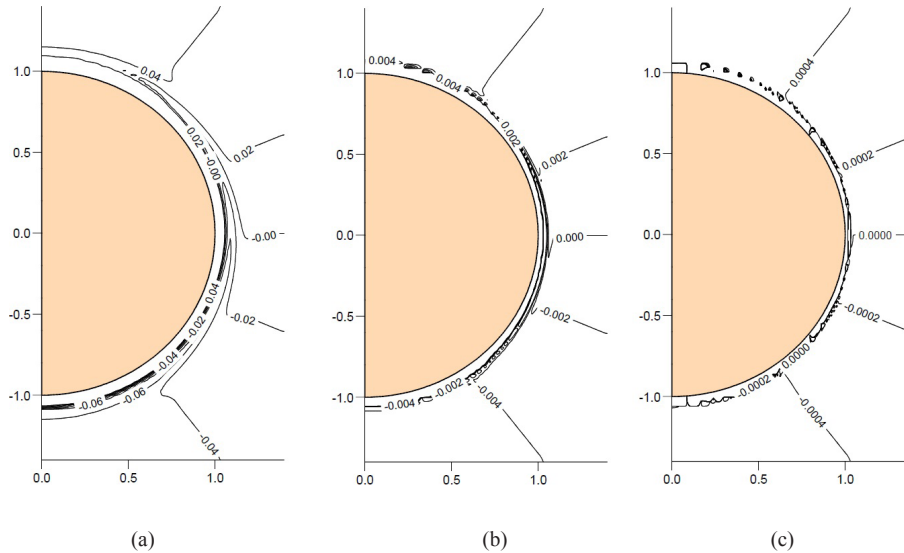


Figure 6. Isotherms of $T^{(i)}$ with $t=1$, $\omega=2$ at (a) $\varepsilon=10^{-1}$ (b) $\varepsilon=10^{-2}$ (c) $\varepsilon=10^{-3}$

The effect of ω is plotted in Fig. 8 for $T^{(i)}$ and Fig. 9 for $\psi^{(i)}$. $T^{(i)}$ diminishes to a steady temperature faster at higher ω . The frequency has effect on the direction of magnitude of $T^{(i)}$, and this persisted as ω increases. From Fig. 8(b), a warmer cap is observed at the upper pole. This shows that the temperature is slightly warmer near the upper vertical axis. However, the major shape of the isotherms remains almost unchanged and the temperature distributes evenly at all angles. This is due to the oscillation effect that heat and cool harmonically. For stream function $\psi^{(i)}$, the magnitude decreases as ω increases. The vortex ring that exists near the horizontal axis moves towards the wall and the shape changes slightly. However, in oscillatory flow the stream function $\psi^{(i)}$ becomes steady at far enough from the wall.

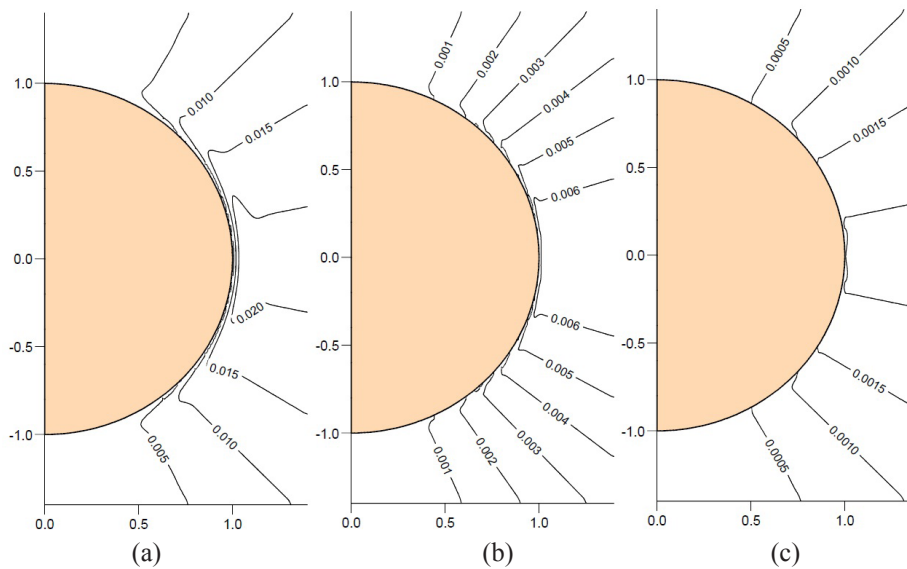


Figure 7. Streamlines of $\psi^{(i)}$ with $t=1$, $\omega=2$ at (a) $\epsilon=10^{-1}$ (b) $\epsilon=10^{-2}$ (c) $\epsilon=10^{-3}$

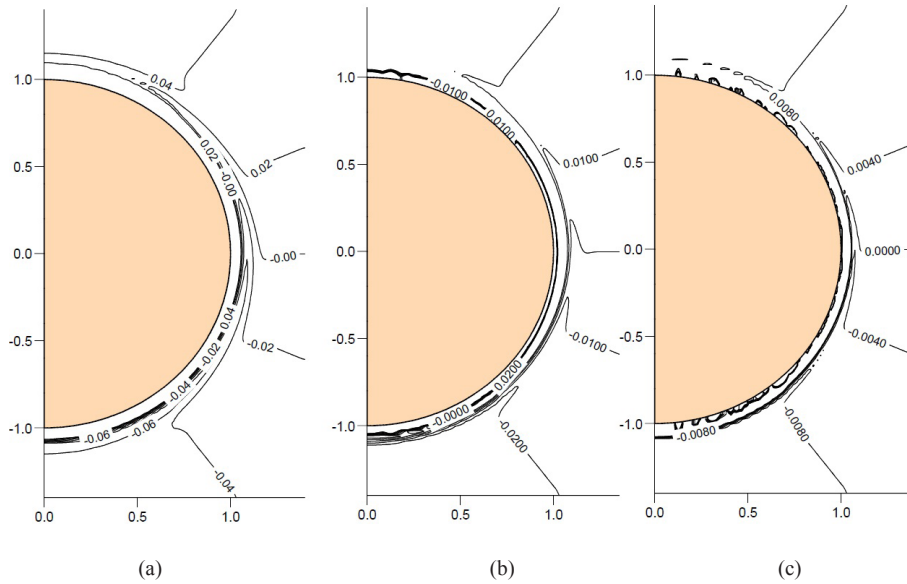


Figure 8. Isotherms of $T^{(i)}$ with $t=1$, $\epsilon=10^{-1}$ at (a) $\omega=2$ (b) $\omega=4$ (c) $\omega=10$

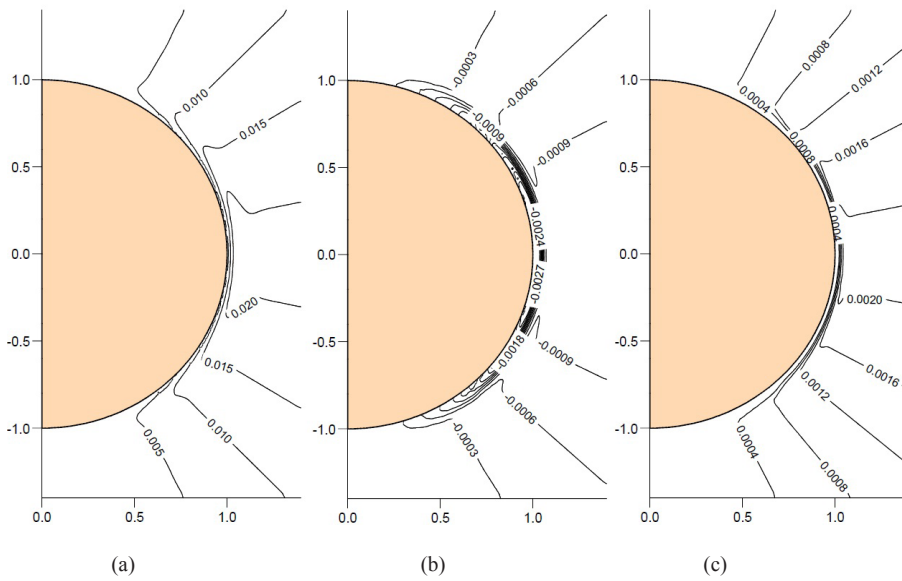


Figure 9. Streamlines of $\psi^{(i)}$ with $t=1$, $\epsilon=10^{-1}$ at (a) $\omega=2$ (b) $\omega=4$ (c) $\omega=10$

4.2 Flow in the outer region

Similar to the previous part, the outer temperature $T^{(0)}$ and stream function $\psi^{(0)}$ are compared by considering different values of frequency ω and the parameter ε in which $Ra=100$. Due to the finite difference method used, the boundary condition at the outer edge far from sphere must be regarded as finite distance. In the present study, the maximum radial coordinate is set at $r=4$.

The temperature $T^{(0)}$ is asymmetrical along the horizontal axis and warmer at the upper pole. No temperature difference is observed along the horizontal axis. Due to the expansion form for temperature $T^{(0)}$ in equation (19), the first-order temperature $T_0^{(0)}$ is of order ε^0 , hence any changes in this parameter will not have significant effect on the temperature. Only stream function $\psi^{(0)}$ that is determined by ε as shown in Fig. 10 but the changes is also not very observable. When ε decreases from 10^{-1} to 10^{-3} , the magnitude of $\psi^{(0)}$ increases slightly but the flow pattern remain almost the same for all ε . $\psi^{(0)}$ is asymmetrical along the horizontal axis but due to the steady value induced from the inner region, $\psi^{(0)}$ executes a negative flow at area very close to the wall. No flow is observed at the vertical axis and the magnitude of $\psi^{(0)}$ increases until maximum at about $\theta=0.471$ inclined from the vertical axis.

Fig. 11 and Fig. 12 shows the changes of $T^{(0)}$ and $\psi^{(0)}$ respectively from $\omega=2$ to $\omega=10$. When ω increases, the temperature $T^{(0)}$ experience a decrease magnitude at all angles. This observation agrees with the solutions obtained from the inner region. A greater change in $T^{(0)}$ is observed near the top and bottom of the sphere, where a thermal plum is

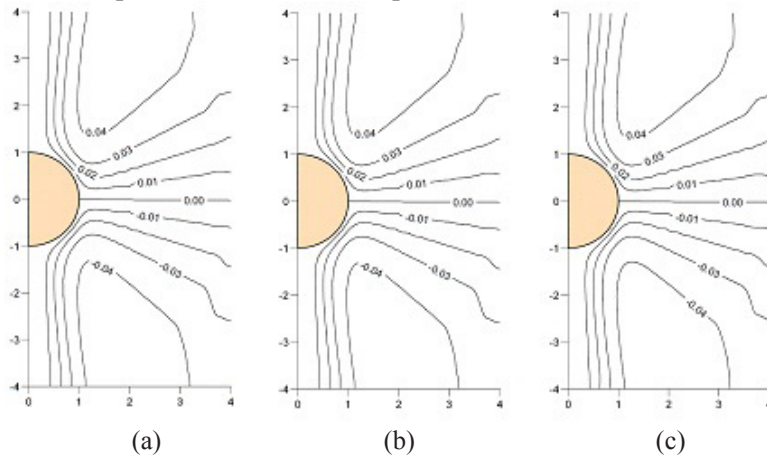


Figure 10. Streamlines of $\psi^{(0)}$ with $\omega=2$ at (a) $\varepsilon=10^{-1}$ (b) $\varepsilon=10^{-2}$ (c) $\varepsilon=10^{-3}$

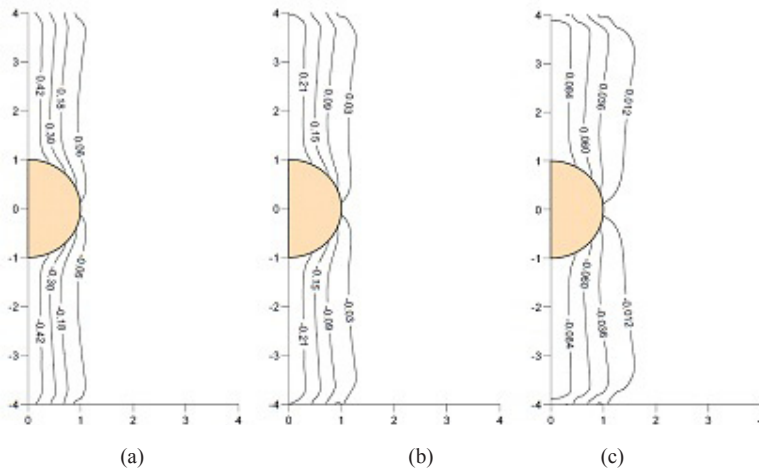


Figure 11. Isotherms of $T^{(0)}$ with $\epsilon=10^{-1}$ at (a) $\omega=2$ (b) $\omega=4$ (c) $\omega=10$

formed. When ω increases, the plume tends to be more parallel to the vertical axis. It is observed that the changes of $T^{(0)}$ due to the oscillatory temperature is more confined near the vertical position about the sphere while the temperature near horizontal position tends to be unaffected. $T^{(0)}$ is also asymmetrical near the horizontal axis. For the stream function, the magnitude of $\psi^{(0)}$ also drops as ω increases and this is mainly due to the steady stream function that forms the boundary condition near the inner edge. As seen from the figure, the flow patterns are almost the same but the magnitude of decreases at both upper part and lower parts of the sphere. The increase of $\psi^{(0)}$ is found to be more rapid for lower ω . And as ω increases the fluid spread outward to the horizontal direction.

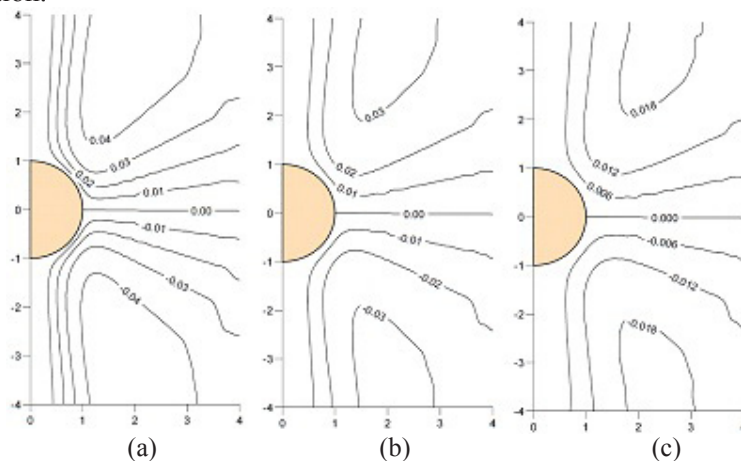


Figure 12. Streamlines of $\psi^{(0)}$ with $\epsilon=10^{-1}$ at (a) $\omega=2$ (b) $\omega=4$ (c) $\omega=10$

5. CONCLUSION

The problem of oscillatory free convection around a sphere in a porous medium has been studied. Other than constant temperature or heat flux problems, it is worthwhile to consider for a sphere immersed in a porous medium and its temperature oscillates harmonically over the surrounding temperature. The matched asymptotic expansion is applied to solve the problem for $Ra=100$. The solution at inner region has been found up to second-order steady term, while the outer region is solved numerically using finite difference method. At both inner region and outer region, the asymptotic expansions for temperature and stream functions are written in the raising order of the parameter $\varepsilon=KU_r/\alpha R_0$.

Motivated by the separation method for second-order steady and unsteady terms in [10], the similar method is applied to the spherical case. Since only the steady terms that are important near the outer region or far from the sphere, by neglecting the unsteady term, the solution is direct to the desire result. At the inner region, it is found that near the outer edge a steady flow is induced, and this agrees with the result obtained by [1, 10]. The condition at the outer edge of this inner layer cannot be satisfied. Therefore, the boundary conditions near the outer region must be matched with the boundary conditions near the outer edge of the inner region. A steady temperature and a steady stream function is found persisted at the outer edge of the inner region, and the steady temperature is not able to satisfy the boundary condition.

The flows when Rayleigh number is 100 are compared in terms of the parameter ε and the frequency parameter ω . It is found generally that as ε decreases, the magnitude of temperature and stream function decreases and the flows are likely to diminish near to the wall of the sphere. While for the increase in frequency ω , the temperature and stream function also tend to drop and diminish near the wall. In the inner region, the magnitude of steady temperature and steady stream function is determined by ω , and only the magnitude of steady stream function that is determined by ε . The unsteady temperature field and stream functions near the inner region are found to be different in terms of the flow pattern with the steady temperature and stream function at the outer region.

Acknowledgement

The author is financially supported by the University Postgraduate Research Scholarship Scheme (PGD) (Ref. No. UMS/CN1.9/B9/18) of the Ministry of Science, Technology and Innovation (MOSTI) and the Fundamental Research Grant Scheme (FRGS) (Grant No. FRG0163-SG2008) , of the Ministry of Higher Education, Malaysia.

REFERENCES

- [1] Merkin, J.H. (1967). "Oscillatory Free Convection from an Infinite Horizontal Cylinder" in *Journal of Fluid Mechanics*, Vol. 30. pp. 561-575.
- [2] Yamamoto, K. (1974). "Natural Convection about a Heated Sphere in a Porous Medium" in *Journal of the Physical Society of Japan*, Vol. 37, No. 4. pp. 1164-1166.
- [3] Cheng, P. (1978). *Heat Transfer in Geothermal Systems. Advances in Heat Transfer, Volume 14.* Academic Press. pp.1-105.
- [4] Chatterjee, A.K. & Debnath, L. (1979). "Double Boundary Layers in Oscillatory Convective Flow" in *Il Nuovo Cimento*, Vol. 52. pp 29-44.
- [5] Ganapathy, R. & Purushothaman, R. (1990). "Free Convection in an Infinite Porous Medium Induced by a Heated Sphere" in *International Journal of Engineering Science*, Vol. 28. No. 8. pp. 751-759.
- [6] Sano, T. & Okihara, R. (1994). "Natural Convection around a Sphere Immersed in a Porous Medium at Small Rayleigh Numbers" in *Fluid Dynamics Research*, Vol. 13. pp. 39-44.
- [7] Yan, B., Pop, I. & Ingham, D.B. (1997). "A Numerical Study of Unsteady Free Convection from a Sphere in a Porous Medium" in *International Journal of Heat and Mass Transfer*. Vol. 40. pp. 893-903.
- [8] Merkin, J.H. & Pop, I. (2000). "Free Convection near a Stagnation Point in a Porous Medium Resulting from an Oscillatory Wall Temperature" in *International Journal of Heat and Mass Transfer*, Vol. 43. pp. 611-621.

- [9] Bejan, A. (2004) *Convective Heat Transfer*. (3rd edition). John Wiley & Sons, New Jersey.
- [10] Rahimi, A.B. & Jalali, T. (2005). "Unsteady Free Convection from a Sphere in a Porous Medium with Variable Surface Temperature" in *International Journal of Engineering*, Vol. 18. pp. 331-350.
- [11] Roslan, R., Hashim, I. & Ghazali, K. (2005). "An Analytical Study of Natural Convection in the Inner Boundary-Layer Subject to Oscillating Temperature" in *Proceeding of International Conference on Applied Mathematics 2005(ICAM05)*. Institut Teknologi Bandung, Bandung, Indonesia. pp. 617-622.
- [12] Lai, Z.P., Roslan, R., Hashim, I. & Zainodin, H.J. (2010). "Inner Solution for Oscillatory Free Convection about a Sphere Embedded in a Porous Medium" in *Proceeding of the 6th IMG-GT Conference on Mathematics, Statistics and its Applications (ICMSA2010)*. Universiti Tunku Abdul Rahman, Kuala Lumpur. pp. 926-934.
- [13] Lai, Z.P., Zainodin, H.J., Hashim, I. & Roslan, R. (2010). "Outer Solution for Oscillatory Free Convection about a Sphere in a Porous Medium" in *Prosiding Seminar Kebangsaan Aplikasi Sains & Matematik 2010, SKASM 2010 sempena Simposium Kebangsaan Sains Matematik ke-18 (SKASM 18)*, 8-10 Disember 2010, The Zone Regency Hotel, Johor Bahru. Jilid 2: Matematik. Universiti Tun Hussein Onn Malaysia, Parit Raja, Johor. pp. 153-161.